Keysight Technologies
Attofarad Capacitance Measurement with Scanning Microwave Microscopy
Application Note

Introduction

Organic thin films have found many applications in molecular electronics, sensors, flexible displays, and photovoltaic devices. The performance of those devices often strongly depends on the quality and homogeneity of the dielectric properties of the organic thin films. However, most of the existing techniques used for dielectric constant measurement are either for bulk materials or averaged over large areas, thus lacking the lateral resolution for localized characterization. Near-field scanning microwave microscopy (NSMM) was one of the techniques developed for quantitative measurement of local complex dielectric constants.[1,2,3] A number of attempts have been made to combine microwave analysis and AFM.[4,5] The most recent development was to combine high precision microwave measurement of a vector network analyzer (VNA) and nanoscale capability of a high performance AFM for localized characterization. Here we demonstrate the application of scanning microwave microscopy (SMM) for the study of organic thin films, using self-assembled monolayers of decanethiol (C10) and octadecanethiol (C18) on Au(111) surface as a model system. The quantitative capacitance measurement was accomplished by carefully calibrating the instrument against a capacitance standard developed by NIST. With such calibration, the capacitances can be measured quantitatively with attofarad resolution.

Experimental

Materials

Decanethiol (C10) and octadecanethiol (C18) are purchased from Sigma-Aldrich, and are dissolved in ethanol, also purchased from Aldrich, to form 0.02 mM of solutions for the preparation of SAM samples. Au(111) substrate is from epitaxial grown Au film on mica.

Instrumentation

The SMM setup includes a 5600LS AFM platform from Keysight and a PNA N5230C network analyzer. Tips used in the experiment are conductive Rocky Mountain Pt cantilevers (RMN 12Pt 400A) with a length of 400 µm, a width of 60 µm, a shank length of 100 µm, and a nominal spring constant of 0.3 N/m. For principles of SMM and its operation please see other application notes from Keysight.[6,7]

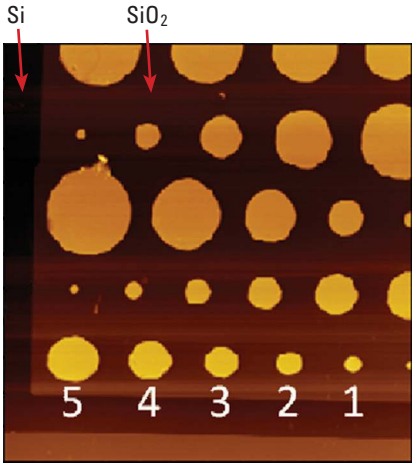

Figure 1. AFM topography image of NIST capacitance standard.

Calibration of SMM using a NIST Capacitance Standard.

The standard sample used for the calibration of absolute capacitance measurement is developed by NIST, it has a series of Au pads of known area deposited on a layer of SiO_2. The thickness of the SiO_2 layer is 50 nm and the substrate is highly doped Si, as shown in Figure 1. The diameters of the row of Au pads labeled 1, 2, 3, 4, and 5 in the image are 1, 2, 3, 4, and 5 micrometers, respectively.

KEYSIGHT TECHNOLOGIES

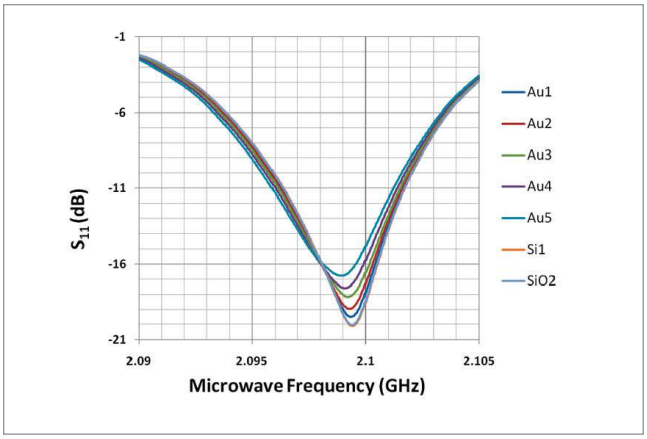

Figure 2. Reflection coefficient S_{11} versus frequency plot measured on different Au pads, Si, and SiO_2.

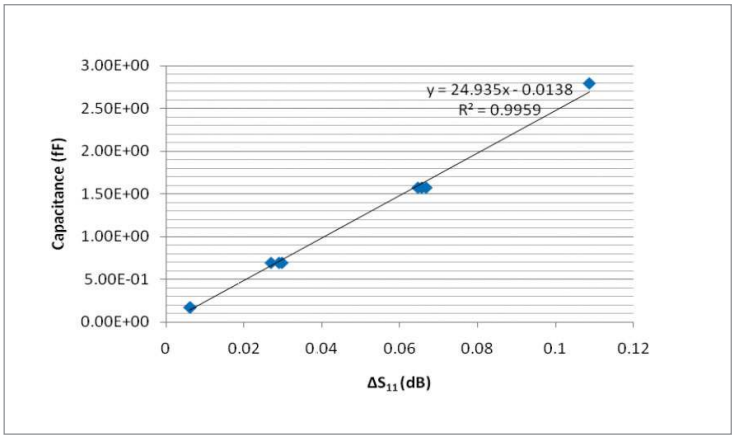

Figure 3. A linear plot of Capacitance against ΔS_{11} with the slope being the calibrated transfer coefficient of the SMM system.

The corresponding capacitances of these structures are 1.82, 4.10, 7.29, 11.40 and 16.41 femtofarads, respectively. SMM measures the impedance at the tip/sample interface by measuring the reflection coefficient S_{11}, as defined by the following equation

$$S_{11} = \frac{Z_L - Z_0}{Z_L + Z_0} \qquad (1)$$

where is the characteristic impedance of the transmission line, typically 50Ω, and is the load impedance, which is equivalent to the impedance at the tip/sample interface in this case. Since the impedance at the tip/sample interface is governed by the capacitance when measuring dielectric thin films, the reflection coefficient S_{11} can be directly correlated to the capacitance, or the dielectric properties of the samples under test. Figure 2 shows the changes of S_{11} as functions of microwave frequency measured on different Au pads. As the Au pad area increases, so does the capacitance, which will in turn cause the S_{11} curve to shift and change in amplitude.

Based on the approach in Reference 4, when the capacitance is small, the change in capacitance and S_{11} follows a linear relationship,

$$\Delta C = k\Delta S_{11} \qquad (2)$$

where is the transfer coefficient of the system that converts the measured S_{11} data to the capacitance change at the tip/sample interface.

During the measurement, the SMM is operated at a fixed frequency, close to the resonance frequency, i.e., the lowest point on the frequency curve shown in Figure 2. Therefore the calibration is also carried out at the same frequency. Figure 3 shows the linear plot between Δ and ΔS_{11} measured at 2.1 GHz which is the operating frequency for this experiment. The plot fits well to a linear regression, suggesting the validity of Equation 2 for capacitance in the femtofarad range.

However, the transfer coefficient cannot be obtained simply from the linear plot in Figure 3. The precisely patterned capacitance structures are made on highly-doped Si substrate, and the dielectric material between the two electrodes is SiO_2; therefore, there always exists an intrinsic capacitance at the SiO_2/Si interface and this capacitance will contribute to the total capacitance that is affecting the S_{11} signal of the system. The exact value of this capacitance is unknown, however, it depends on the size of the Au pad but not the thickness of the SiO_2 layer.[8] Since the total capacitance can be seen as two components in serial, i.e., the capacitance of the Au/SiO_2/Si and that of the SiO_2/Si , the total capacitance can be expressed as

$$1/C_{total} = 1/C_{pad} + 1/C_{ox} \qquad (3)$$

and,

$$1/\Delta S_{11} = k/C_{total} = k/C_{pad} + k/C_{ox} = kd/(\varepsilon_r \varepsilon_0 A) + const \qquad (4)$$

Therefore, the transfer coefficient can be obtained from a plot of the measured PNA signal ($1/\Delta S_{11}$) against the thickness of the SiO_2 film , provided the measurements are all done with Au pads of the same area. For a detailed study on SMM calibration for absolute capacitance measurement, one is referred to the work done in Reference 8.

The structure designed for such calibration are shown in Figure 4, which consists of Au pads of different sizes deposited on SiO_2 layers of different thickness. The nominal diameters of these Au pads are 1, 2, 3, and 4 µm, and the thickness of the SiO_2 layers are 50, 100, 150, and 200 nm, respectively. The Au pads on the same row are of the same size, e.g., the row of Au pads along the profile line all have a nominal area of 7.07 μm^2. A simple GUI for capacitance calibration is provided in PicoView. Based on Equation 4, the

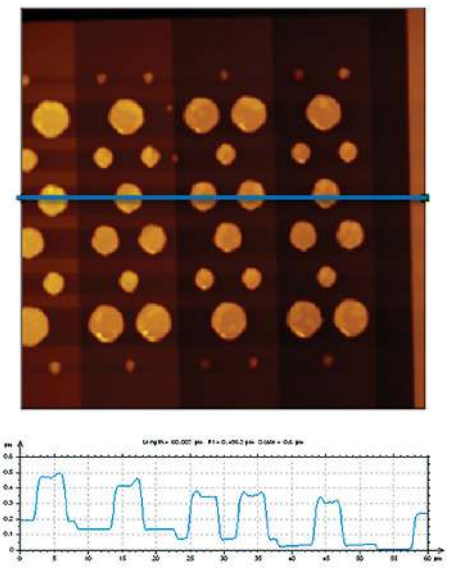

Figure 4. Standard capacitance structure for SMM calibration, which consists of a Au pads of well defined area deposited on SiO_2 films of precise thickness.

calibration is done by measuring the S_{11} amplitude against the SiO_2 background for Au pads of the same size sitting on different SiO_2 steps, i.e., the Au pads on the same row across different SiO_2 layers. After putting the measured data and the area of the Au pads used for measurement into the window, the inversed PNA amplitude ($1/\Delta S_{11}$) is plotted against the film thickness to obtain the transfer coefficient, . A screenshot of the capacitance calibration window from PicoView is presented in Figure 5.

Preparation of C18/C10 Mixed SAM Layers.

The pattern formed by C18 within C10 self-assembled monolayer matrix on Au surface is generated by a method known as Nanografting.[9] The Au substrate was first immersed into the C10 thiol solution. The C10 thiol molecules initially absorb onto gold with the hydrocarbon chains oriented parallel to the substrate. When the surface coverage of this so-called lying-down phase increases to near saturation, continuous collisions by thiols from solution induce a lateral pressure and lead to a two dimensional phase transition, during which thiols reorient from an intermediate lying-down state to the ultimate standing up configuration. Since the activation energy of the phase transition step for organothiols with a single SH group is moderate, molecules can overcome the energy barrier and convert to an upright monolayer readily at room temperature. After the C10 SAM layer was formed, the sample was put under an AFM tip in a liquid cell containing C18 thiol molecules. An area on the surface was scanned with high force and the C10 molecules under impact were removed from the surface. The freshly exposed area of gold is confined by the surrounding undisturbed matrix molecules. Under controlled conditions, it can be covered by the abundant C18 thiol molecules to form a restricted SAM layer inside the C10 matrix. Then the surface was dried with N_2 gas and setup for SMM imaging. As shown by the friction image (Figure 6B), a 2x2 µm pattern of C18 inside C10 matrix was created by nanografting. The structure of the compact monolayer of those thiol molecules on Au surface has been well characterized. The thickness of the C10 SAM layer is 1.32 nm while that of the C18 SAM layer is about 2.2 nm, resulting in a height difference of 0.9 nm between the two layers. Since the height difference is small, it is not clearly visible in the topography image (Figure 6A), however, the difference between the two SAM layers is clearly visible in the friction image.

Capacitance measurement on C18/C10 mixed SAM layers

Figure 6C and 6D shows the amplitude and phase images of the S_{11} signal measured simultaneously with the topography and the friction. The reflection coefficient, as suggested by Equation (1), is complex by definition. Its phase angle indicates the contribution from nonlinear components of the device under test. In our case, it is related to the capacitance nature at tip and sample interface. Both of the amplitude and phase images clearly revealed the difference between the C10 and C18 SAM layers, it is the amplitude signal will be used to calculate the quantitative capacitance difference. As seen from Figure 1, an increase in the capacitance causes the S_{11} curve to shift upwards and to a lower frequency. At the constant frequency used for this measurement, the S_{11} signal will increase with capacitance. Because the dielectric constant of the two thiol molecules are quite the same, the thicker C18 SAM layer will give a smaller capacitance comparing to the thinner C10 SAM layer. Consequently, the image in Figure 6C shows a darker 2x2 µm area for the C18 SAM layer and a brighter contrast for the surrounding C10 SAM layer.

The phase image (Figure 6D) shows a reversed contrast comparing to the amplitude image. It needs to be pointed out that the changes in the phase of the S_{11} signal also strongly depends on the microwave frequency, and it is difficult to interpret the contrast in the phase image without this knowledge.

The relative dielectric constant of alkane thiols has been reported to be ~2.0, and varies little with the length of the carbon chain.[10] Assuming C10 and C18 thiols has the same relative dielectric constant, then the capacitance difference measured between the two SAM layers is only caused

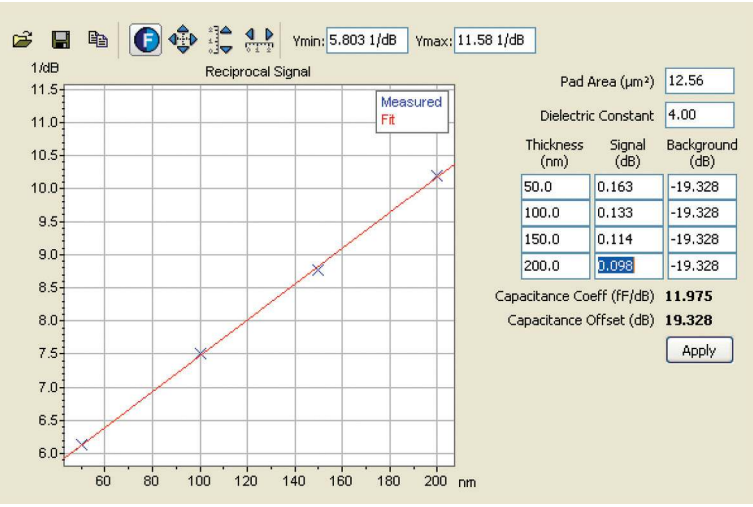

Figure 5. Screenshot of the capacitance calibration GUI in PicoView. The transfer coefficient of the SMM system is calculated from the linear plot of $1/\Delta S_{11}$ vs d, the thickness of the SiO_2 layer.

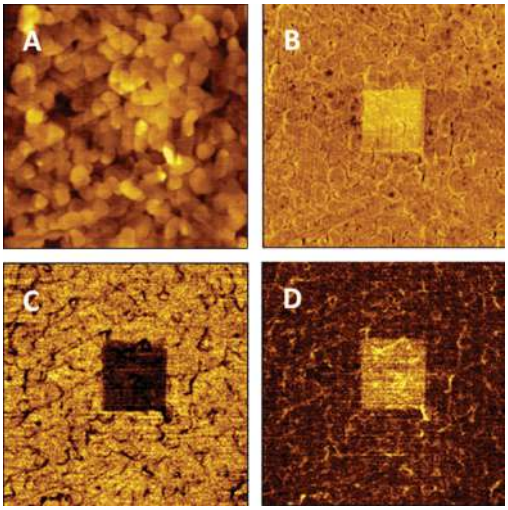

Figure 6. SMM imaging of a C18/C10 SAM structure on Au(111) surface: A) topography, B) friction, C) S_{11} amplitude, and D) S_{11} phase.

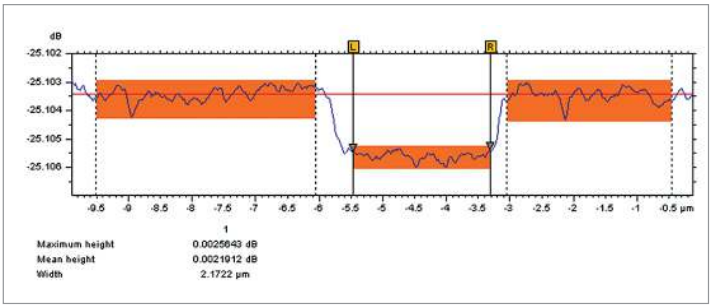

Figure 7. Difference in S_{11} amplitude between the C10 and C18 SAM layers measured from the horizontal profile drawn from Figure 6C.

by the difference in thickness, according to Equation 4. The average difference in S_{11} measured from the image in Figure 6C is about 0.002 dB, corresponding to 24 aF in capacitance difference. A line profile from Figure 6C is presented in Figure 7, illustrating the calculation of $\Delta\Delta S_{11}$ from the measured S_{11} amplitude. Since the contact area between the tip and sample is much larger compared to the thickness of those SAM layers, one can assume the tip sample interface acts like a simple parallel plate capacitor. The thickness of the C10 and C18 SAM layers are 1.3 nm and 2.2 nm, respectively, therefore, the effective contact area between the tip and the sample in this experiment can be estimated to be about 60 nm in diameter.

Conclusions

Scanning microwave microscopy can be used to study the dielectric properties of organic thin films, including self-assembled monolayers of organic molecules. As demonstrated in this work, with a careful calibration, SMM can detect attofarad range of small capacitance difference across the organic film. With the knowledge of the film thickness from a material of known relative dielectric constants, the effective contact area between the tip and the sample can be estimated based on established models. From the C10 and C18 SAM structure generated by nanografting, the effective contact area between the probe and the sample surface in this work is estimated to be about 60 nm in diameter. This knowledge of effective contact area can then be applied to measure dielectric constants of other films, or film thickness, etc., using the same probe.

Acknowledgements.

The authors would like to thank Dr. Hassan Tanbakuchi of Keysight for technical discussions.

References

1. Chen, L.F.; Ong, C.K.; Neo, C.P.; Varadan, V.V.; Varadan, V.K. *Microwave Electronics,* John Wiley & Sons, 2004.
2. Gao, C.; Xiang, X.D. *Rev. Sci. Instrum.* 1998, 3846.
3. Tabib-Azar, M.; Akinwande, D.; Ponchak, G.; LeClair, S.R. *Rev. Sci. Instrum.* 1999, 3381.
4. Karbassi, A.; Ruf, D.; Bettermann, A.D.; Paulson, C.A.; van der Weide, D.W; Tanbakuchi, H.; Stancliff, R. *Rev. Sci. Instrum.* 2008, 094706.
5. Rosner, B.T.; van der Weide, D.W. *Rev. Sci. Instrum.* 2002, 2505.
6. Han, W. *Application Note 5989-8881 "Introduction to Scanning Microwave Microscopy",* Keysight, 2014.
7. Serry, F.M. *Application Note 5989-8818 "Scanning Microwave Microscope",* Keysight, 2014.
8. Huber H-P; Moertelmaier, M.; Wallis, T.M.; Chiang, Chin-Jen; Hochleitner, M.; Imtiaz, A.; Oh, Yoo Jin; Schilcher, K.; Dieudonne, M.; Smoliner, J.; Hinterdorfer, P.; Rosner, S.J.; Tanbakuchi, H.; Kabos, P; Kienberger, F. *Rev. Sci. Instrum.* Submitted.
9. Xu, S.; Liu, G.Y. *Langmuir* 1997, 127.
10. Akkerman, H.B.; Naber, R.C.G.; Jongbloed, B.; van Hal, P.A.; Blom, P.W.M.; de Leeuw, D.M. *PNAS* 2007, 11161.

For more information on Keysight Technologies' products, applications or services, please contact your local Keysight office. The complete list is available at: www.keysight.com/find/contactus

Americas

Canada	(877) 894 4414
Brazil	55 11 3351 7010
Mexico	001 800 254 2440
United States	(800) 829 4444

Asia Pacific

Australia	1 800 629 485
China	800 810 0189
Hong Kong	800 938 693
India	1 800 112 929
Japan	0120 (421) 345
Korea	080 769 0800
Malaysia	1 800 888 848
Singapore	1 800 375 8100
Taiwan	0800 047 866
Other AP Countries	(65) 6375 8100

Europe & Middle East

Austria	0800 001122
Belgium	0800 58580
Finland	0800 523252
France	0805 980333
Germany	0800 6270999
Ireland	1800 832700
Israel	1 809 343051
Italy	800 599100
Luxembourg	+32 800 58580
Netherlands	0800 0233200
Russia	8800 5009286
Spain	0800 000154
Sweden	0200 882255
Switzerland	0800 805353 Opt. 1 (DE) Opt. 2 (FR) Opt. 3 (IT)
United Kingdom	0800 0260637

For other unlisted countries:
www.keysight.com/find/contactus
(BP-07-10-14)

www.keysight.com/find/afm

KEYSIGHT TECHNOLOGIES

This information is subject to change without notice.
© Keysight Technologies, 2010 - 2014
Published in USA, July 31, 2014
5990-5702EN
www.keysight.com